Scanning Gate Microscopy of a Nanostructure where Electrons Interact

Axel Freyn, Ioannis Kleftogiannis, Jean-Louis Pichard

Scanning Gate Microscopy of a Nanostructure where Electrons Interact

Axel Freyn, Ioannis Kleftogiannis,* and Jean-Louis Pichard
Service de Physique de l'État Condensé (CNRS URA 2464), DSM/IRAMIS/SPEC, CEA Saclay, 91191 Gif-sur-Yvette Cedex, France

Two dimensional electron gases created in semiconductor heterostructures are contacted via a nanostructure. The density is locally changed by a charged tip which can be moved in the vicinity of the nanostructure. Scanning gate microscopy consists in making images giving the quantum conductance of this setup as a function of the tip position. From those images, we show that the strength of electron-electron interactions inside the nanostructure can be measured.

PACS numbers: 07.79.-v,71.10.-w,72.10.-d,73.23.-b

Semiconductor nanostructures based on two dimensional electron gases (2DEGs) have been extensively studied, with the expectation of developing future devices for sensing, information processing and quantum computation. However, fundamental aspects of electron-electron interactions have been neglected till now in low temperature scanning gate microscopy (SGM) of such nanostructures. Those aspects are studied in this letter, assuming a SGM setup (FIG. 1) which was used in Refs. [1, 2], the nanosystem being a quantum point contact (QPC) which exhibits conductance plateaus multiple of $g_q = 2e^2/h$ as the contact is progressively closed. The quantum conductance g is measured between the two ohmic contacts and the effect of the charged tip of an AFM cantilever upon g is studied as a function of the tip position. The negatively charged tip capacitively couples with the 2DEG, creating a depletion region that scatters the electrons. For $g \approx g_q$, the charged tip can reduce [2] g by a significant fraction δg, which falls off with distance r_T from the QPC. Moreover, fringes spaced by $\lambda_F/2$, half the Fermi wave length, can be seen in the experimental images giving δg as a function of the tip position. Very small distances r_T were not scanned in Ref. [1, 2], but this was done [3] later, giving extra ring structures inside the QPC if g is biased between the conductance plateaus. Though many features of the SGM images can be described by theories [4, 5] neglecting the many body effects inside the QPC, we will show that signatures of these effects should be observed in the vicinity of the QPC. Therefore, from the SGM images, one can detect if the electrons interact inside the QPC. Two main signatures of the interaction have been identified: fringes of enhanced magnitude, falling off as $1/r_T^2$ near the QPC, before falling off as $1/r_T$ far from the QPC, and a phase shift of the fringes between these two regions. An almost closed QPC, around the $0.7g_q$ conductance anomaly [6], should be a relevant interacting nanosystem to study. However, our theory is more general and applies to any nanosystem inside which electrons interact.

SGM consists in scanning the tip around the nanosystem and in making images of $\delta g = g - g_0$, g (g_0) being the conductance with (without) tip. Without interaction, the nanosystem transmission is independent of the tip position, and the SGM images reveal the interferences of electrons which are transmitted by the nanosystem and elastically backscattered by the tip through the nanosystem. If the transmitted and backscattered flows interact inside the nanosystem, the interferences become more subtle, because the effective nanosystem transmission depends on the tip position. The origin of this interaction effect is easy to explain [7, 8, 9] if one uses the Hartree-Fock (HF) approximation. The tip induces Friedel oscillations of the electron density, which can modify the density inside the nanosystem. As one moves the tip, this changes the Hartree corrections of the nanosystem and its effective transmission, while a related effect characterizes also the Fock corrections [7, 8, 9]. For a non interacting nanosystem, the SGM images depend only on quantum interferences occurring at the Fermi Energy E_F. For an interacting nanosystem, this is no longer true, as the HF corrections, and hence the effective nanosystem transmission, depend on interferences taking place at all energies below E_F.

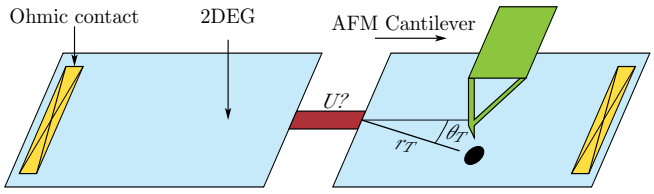

FIG. 1: Scheme of a SGM setup: Two 2DEGs are connected via a nanostructure (red). The negatively (positively) charged tip creates a small depletion (accumulation) region (•) which scatters electrons in the right 2DEG. By scanning the tip and measuring the quantum conductance g between the 2 ohmic contacts, one can detect the interaction U acting inside the nanostructure.

The principle for the detection of the interaction U via SGM can be simply explained in one dimension, the nanosystem being coupled to semi-infinite chains. If $U = 0$, the transmitted flow interfers with the flow reflected by the tip, giving rise to Fabry-Pérot oscillations which do not decay as $r_T \to \infty$. Hence the conductance g of the nanosystem in series with the tip exhibits oscillations which do not decay. If $U \neq 0$, the nanosystem

HF-corrections are modified by the Friedel oscillations induced by the tip inside the nanosystem. This gives an additional effect for g, which decays as the Friedel oscillations causing it ($1/r_T$-decay in 1d, with oscillations of period $\lambda_F/2$). Measuring g as a function of the tip position, one gets oscillations of period $\lambda_F/2$ in the two cases, but their decays are different and allow to measure the interaction strength U inside the nanosystem.

Interactions in 1d chains give rise to a Luttinger-Tomonaga liquid and cannot be neglected. It is necessary to take 2d strips of sufficient electron density (factor $r_s < 1$) for neglecting interaction outside the nanosystem. The effect of the tip becomes more subtle with 2d strips: First, the Friedel oscillations decreasing as $1/r^d$ in d dimensions, the effect of the tip upon the nanosystem transmission has a faster decay, unless focusing effects take place. Second, the non interacting limit becomes more complicated. The probability for an electron of energy E_F to reach the tip, and to be reflected through the nanosystem also decays as $r_T \to \infty$. Assuming isotropy, the probabilities of these two events should decay as $1/r_T$, giving a total $1/r_T^2$ decay for δg. But isotropy is not a realistic assumption for SGM setups. The transmission can be strongly focused, making the effect of the tip a function of the angle θ_T. Spectacular focusing effects have been observed [1] using a QPC: The effect of the tip is mainly focused around $\theta_T \approx 0$ or $\pm\pi/4$, depending if $g_0 \approx g_q$ or $2g_q$.

For studying SGM with 2d strips more precisely, we use a simple model sketched in FIG. 2 (upper left), assuming spin polarized electrons (spinless fermions). The Hamiltonian reads $H = H_{\rm nano} + H_{\rm strips} + H_T$.

$$H_{\rm nano} = V_G \sum_{x=0}^{1} n_{x,0} - t_d(c^\dagger_{0,0}c_{1,0} + H.c.) + U n_{0,0}n_{1,0} \quad (1)$$

describes a nanosystem with two sites of energy V_G and of hopping term t_d. We assume that V_G can be varied by an external gate. A repulsion of strength U acts between these two sites. $c_{x,y}$ ($c^\dagger_{x,y}$) is the annihilation (creation) operator at site x, y, and $n_{x,y} = c^\dagger_{x,y}c_{x,y}$.

$$H_{\rm strips} = -t_{\rm h} \sum_{x,y} (c^+_{x,y}c_{x,y+1} + c^+_{x,y}c_{x+1,y} + H.c.) \quad (2)$$

describes the strips and their couplings to the nanosystem. The left (right) strip occupies the sites with $-L_y \le y \le L_y$ and $-\infty \le x \le 0$ ($1 \le x \le \infty$), if ones excepts the two nanosystem sites. We assume hard wall boundaries in the y-direction. $t_{\rm h} = 1$ sets the energy scale. $H_T = V_T n_{x_T,y_T}$ describes the effect of a tip located above a site of coordinates $(x_T > 1, y_T) = r_T(\cos\theta_T, \sin\theta_T)$.

FIG. 2 (upper right) shows how one can use SGM for detecting U in the 1d limit of our model ($L_y = 0$). The chains are half-filled ($E_F = 0$), and the conductance g of the nanosystem in series with a tip is given as a function of r_T. If $U = 0$, g exhibits even-odd oscillations

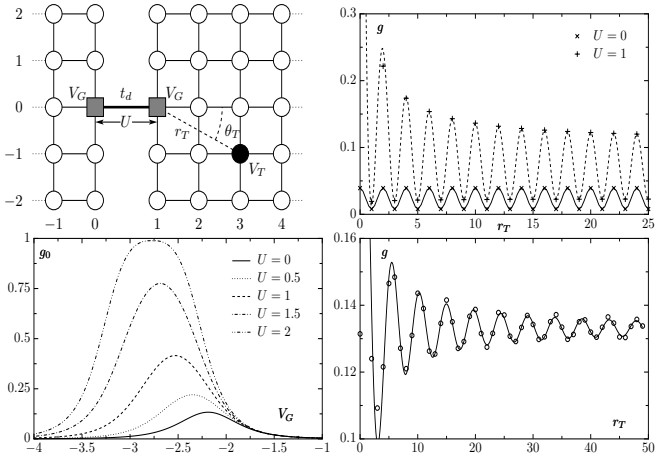

FIG. 2: Upper left: Used SGM setup: 2 strips of width $2L_y + 1$ (here $L_y = 2$) are connected via a nanosystem (2 sites □, hopping t_d and potentials V_G). The repulsion U acts only inside the nanosystem. The charged tip gives rise to a potential V_T (•) at a distance r_T from the nanosystem. Upper right: SGM measure using 1d chains ($L_y = 0$) at half-filling ($k_F = \pi/2$), giving the conductance g of the nanosystem ($V_G = -U/2$ and $t_d = 0.1$) in series with a tip ($V_T = 2$) as a function of r_T. Fits $0.024 + 0.016\cos(\pi r_T)$ (solid line) and $0.066 + 0.132/r_T + (0.043 + 0.014/r_T)\cos(\pi r_T)$ (dashed line). Lower left: Conductance g_0 without tip ($V_T = 0$) as a function of V_G for 2d strips ($2L_y + 1 = 301$). $E_F = -3.57$ ($k_F = 0.668$), $t_d = 0.1$ and different values of U. Lower right: g as a function of r_T, showing a $1/r_T$-decay of δg when $U = 0$. $\theta_T = 0$, $t_d = 0.1$, $V_G = -2.187$, $V_T = -2$, $E_F = -3.57$ and $2L_y + 1 = 301$. Solid line: $0.133 + 0.110\cos(2k_F r_T - 1.2)/r_T$.

of constant amplitude, while these oscillations fall off as $1/r_T$ near the nanosystem if $U \neq 0$. When $L_y = 0$, the HF corrections can be obtained using an extrapolation method [7, 8, 9]. When L_y is large, using self-energies becomes more efficient for calculating the HF corrections and the conductance g. Hereafter, we summarize the used method for calculating the SGM images.

In the Landauer approach to transport, it is convenient to separate the measured system, the leads and their couplings. All the sites x, y for which $0 \le x \le x_T$ define the measured system (nanosystem + tip) of Hamiltonian H_S. All the sites for which $-\infty < x \le -1$ ($x_T + 1 \le x < \infty$) define the left (right) lead of width $2L_y + 1$. The system and the leads are coupled by hopping terms of amplitude $t_{\rm h}$. In the zero temperature limit, the Landauer conductance g (in units of e^2/h for spinless fermions) reads [10]

$$g = \text{trace}\left[\Gamma^{(L)}\langle 0|G^a_S|x_T\rangle\Gamma^{(R)}\langle x_T|G^r_S|0\rangle\right]_{E=E_F}. \quad (3)$$

$$G^{r,a}_S = \left[z - H_S - \Sigma^T - \Sigma^{\rm HF}\right]^{-1}, \quad (4)$$

are the retarded ($z = E + i\eta$) and advanced ($z = E - i\eta$) Green's functions of the measured system at an energy E, $\eta \to 0^+$. $\Sigma^T = \Sigma^L + \Sigma^R$. $\langle x_1|G^{r,a}_S|x_2\rangle$ are $(2L_y + 1) \times$

$(2L_y+1)$ matrices giving the elements of $G_S^{r,a}$ evaluated between the sites x_1, y and x_2, y'. The expressions of the $(2L_y+1)\times(2L_y+1)$ matrices $\Sigma^{L,R}$ and $\Gamma^{L,R}$ induced by coupling the measured system to the left (L) and right (R) leads can be found in the literature [10].

Since the electrons interact only inside the nanosystem, the HF self-energy $\Sigma^{\rm HF}$ is a matrix with only 4 non zero matrix-elements $\Sigma^{\rm HF}_{\mathbf{i},\mathbf{j}} = \langle i,0|\Sigma^{\rm HF}|j,0\rangle$ where $i,j=0,1$. The diagonal elements give the 2 Hartree self-energies $\Sigma^{\rm H}_{\mathbf{i},\mathbf{i}}$, $\mathbf{i}=\mathbf{0},\mathbf{1}$ while the off-diagonal elements give the Fock self-energy $\Sigma^{\rm F}_{\mathbf{0},\mathbf{1}} = \Sigma^{\rm F}_{\mathbf{1},\mathbf{0}}$. To calculate the HF self-energies, one needs only the Green's function inside the nanosystem (2×2 matrix $g_{\rm nano}$), which depends on the self-energies σ_L ($\sigma_R(V_T)$) describing the effect of coupling the left strip (right strip with the tip) to the nanosystem site $\mathbf{0}=(0,0)$ ($\mathbf{1}=(1,0)$). If $G^{L,R}_{\rm strip}$ are the Green's functions of the left (right) strips excluding the 2 nanosystem sites, one gets

$$\sigma_{L,R} = \sum_{I,J}\langle I|G^{L,R}_{\rm strip}|J\rangle. \tag{5}$$

I and J label the 3 sites $(2,0),(1,1)$ and $(1,-1)$ directly coupled to $\mathbf{1}$ for $\sigma_R \equiv \sigma_{\mathbf{1}}$ ($(-1,0),(0,1)$ and $(0,-1)$ coupled to $\mathbf{0}$ for $\sigma_L \equiv \sigma_{\mathbf{0}}$). $\sigma_{\mathbf{1}}$ is a function of the tip position which we calculate using recursive Green's function (RGF) algorithm (see Ref. [5] and references therein).

$g_{\rm nano}$ being given by $(g^{-1}_{\rm nano})_{\mathbf{i},\mathbf{i}} = z - V_G - \sigma_{\mathbf{i}} - \Sigma^{\rm HF}_{\mathbf{i},\mathbf{i}}$ and $(g^{-1}_{\rm nano})_{\mathbf{i},\mathbf{j}\neq\mathbf{i}} = t_d - \Sigma^{\rm HF}_{\mathbf{i},\mathbf{j}}$ for $z = E + i\eta$, the HF self-energies are the self-consistent solution of 3 coupled integral equations:

$$\Sigma^{\rm H}_{\mathbf{0},\mathbf{0}} = -\tfrac{U}{\pi}\Im\int_{-\infty}^{E_F}(g_{\rm nano}(E))_{\mathbf{1},\mathbf{1}}dE \tag{6}$$

$$\Sigma^{\rm H}_{\mathbf{1},\mathbf{1}} = -\tfrac{U}{\pi}\Im\int_{-\infty}^{E_F}(g_{\rm nano}(E))_{\mathbf{0},\mathbf{0}}dE \tag{7}$$

$$\Sigma^{\rm F}_{\mathbf{0},\mathbf{1}} = \tfrac{U}{\pi}\Im\int_{-\infty}^{E_F}(g_{\rm nano}(E))_{\mathbf{0},\mathbf{1}}dE. \tag{8}$$

The numerical calculations involve successive steps: Eqs. (6-8) are integrated using Cauchy theorem and taking a semi-circle centered at $(E_F-4)/2$ in the upper part of the complex plane. The integration is done using the Gauss–Kronrod algorithm. This requires to calculate $g_{\rm nano}$ (and therefore $\sigma_{\mathbf{i}}$) for 87 complex energies z on the semi-circle, before determining the self-consistent solutions of Eqs. (6-8) recursively. In the presence of the tip in the right strip ($V_T\neq 0$), $\langle I|G^R_{\rm strip}|J\rangle$ giving $\sigma_{\mathbf{1}}$ are calculated using RGF algorithm. Once the matrix $\Sigma^{\rm HF}$ is obtained, one gets g (Eq. 3) using RGF algorithm to calculate $\langle 0|G^a_S(E_F)|x_T\rangle$ and $\langle x_T|G^r_S(E_F)|0\rangle$ in the presence of the tip.

For having negligible lattice effects and SGM images characteristic of the continuum limit, we consider a low filling factor $\nu\approx 1/25$ in the 2d strips, corresponding to a Fermi energy (momentum) $E_F=-3.57$ ($k_F=0.668$). Moreover, we take small values of the nanosystem hopping t_d, in order to increase [8, 9] the effect of the tip upon the nanosystem transmission. FIG. 2 (lower left) gives g_0 as a function of V_G for increasing values of U. When t_d is small, the double peak structure of $g_0(V_G)$ characteristic of a nanosystem with two sites merges [9] to form a single peak. Hereafter, we will always determine the value $V_0(U)$ of V_G for which $g_0(V_G)$ is maximum (FIG. 2 lower left), and the SGM images will be always studied at $V_G = V_0(U)$. FIG. 3 (a) gives $\delta g/g_0$ ($\delta g = g(V_T=-2)-g_0$) as a function of the tip position (x_T,y_T) when $U=0$. One can see that δg decays as r_T increases, the image exhibiting fringes spaced by $\lambda_F/2$. The decay depends on the angle θ_T. For $\theta_T=0$, one can see in FIG. 2 (lower right) that δg falls off as $1/r_T$, and not as $1/r_T^2$ (isotropic assumption). The data are fitted by a function

$$F(r_T) = \frac{a_1\cos(2k_Fr_T+\delta_1)}{r_T} + \frac{a_2\cos(2k_Fr_T+\delta_2)}{r_T^2}, \tag{9}$$

which contains 4 adjustable parameters a_1,δ_1,a_2 and δ_2. The $\cos(2k_Fr_T+\delta)$ terms give fringes spaced by $\lambda_F/2$. The $1/r_T$ term turns out to describe $g(r_T)$ without interaction. This is shown in FIG. 2 (lower right), a function

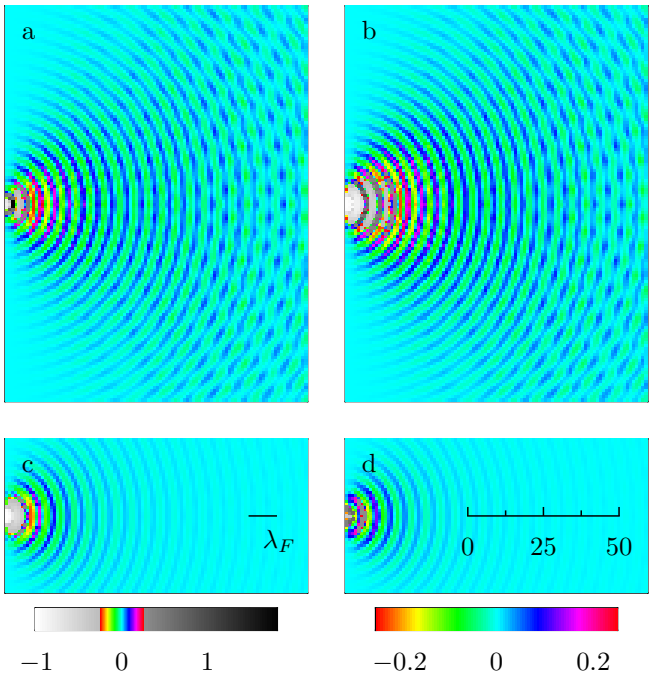

FIG. 3: Images obtained by scanning the tip ($V_T=-2$) on the right strip for $E_F=-3.57$, $t_d=0.01$ and strips of width $2L_y+1=301$. $V_G=-2.870$ (-2.187) is chosen such that $g_0(V_G)=0.188$ (0.0014) is maximum for $U=1.7$ ($U=0$). The Fermi wave length λ_F and the scale are given in FIG. (c) and (d) respectively. Relative corrections $\delta g/g_0$ for $U=0$ (FIG. a) and $U=1.7$ (FIG. b). Relative corrections $\delta\Sigma^{\rm F}/\Sigma^{\rm F}_0$ (FIG. c) and $\delta\Sigma^{\rm H}/\Sigma^{\rm H}_0$ (FIG. d) of the Fock and Hartree self-energy (left nanosystem site) for $U=1.7$. $\delta\Sigma=\Sigma-\Sigma_0$, Σ_0 characterizing the setup without tip ($V_T=0$). $\Sigma^{\rm F}_0=-0.120$. $\Sigma^{\rm H}_0=0.529$.

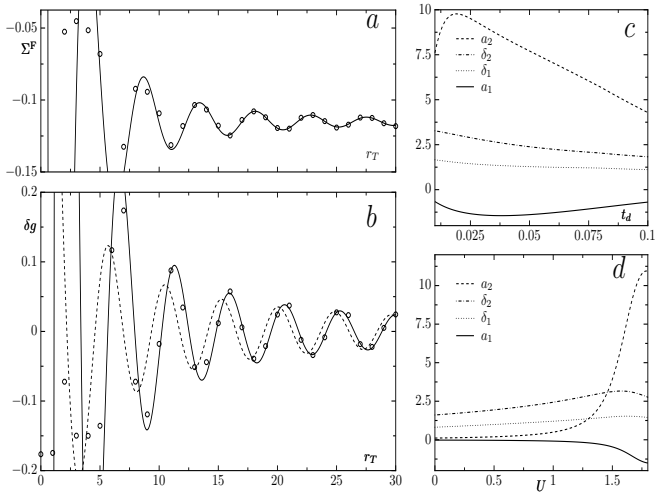

FIG. 4: $\theta_T = 0, E_F = -3.57, U = 1.7, 2L_y + 1 = 301$ and $t_d = 0.01$, V_G chosen such that $g_0(V_G)$ is maximum for the considered values of U and t_d. FIG. a: $1/r_T^2$ decay of the Fock self-energy $\Sigma^F_{0,1}$ ($\circ$) as a function of r_T. Solid line: $-0.115 + 2.379\cos(2k_F r_T + 0.765)/r_T^2$. FIG. b: δg ($g_0 = 0.177$) as a function of r_T ($\circ$). Fit $F(r_T)$ with $a_1 = -0.676$, $a_2 = -7.605$, $\delta_1 = 1.664$ and $\delta_2 = 0.120$ (solid line). Taking $a_2 = 0$ in $F(r_T)$ (dashed line) fails to describe δg below $r_T \approx 30$. FIG. c: Parameters of $F(r_T)$ fitting δg as a function of t_d when $U = 1.7$. FIG. d: Parameters of $F(r_T)$ fitting δg as a function of U when $t_d = 0.02$.

$F(r_T)$ with only two non zero parameters a_1 and δ_1 fitting $\delta g(r_T)$ when $U = 0$. When $U \neq 0$, assuming Friedel oscillations decaying as $\cos(2k_F r_T + \delta)/r_T^2$ in 2d leads, a second term $a_2\cos(2k_F r_T + \delta_2)/r_T^2$ must be added to $F(r_T)$ to describe the effect of the tip upon g occurring via the HF self-energies.

When $U = 1.7$ and $t_d = 0.01$, FIGs. 3 (c and d) show the effect of the tip upon the HF self-energies $\Sigma^{\rm HF}$. The images show fringes spaced by $\lambda_F/2$ which fall off as $1/r_T^2$, as expected since they are driven by 2d Friedel oscillations. The $1/r_T^2$ decay of the Fock term $\Sigma^{\rm F}$ is shown in FIG. 4 (a). We have obtained a similar decay for the 2 Hartree terms. FIG. 3 (b) gives the corresponding SGM image of the conductance g. Near the nanosystem, the effect of the tip upon $\Sigma^{\rm HF}$ is important and yields a $1/r_T^2$ decay of $\delta g(r_T)$. Far from the nanosystem, the effect of the tip upon $\Sigma^{\rm HF}$ is negligible and we expect that $\delta g(r_T)$ falls off as when $U = 0$ ($1/r_T$ decay). As r_T increases, a crossover from a decay described by the term $a_2\cos(2k_F r_T + \delta_2)/r_T^2$ of $F(r_T)$ towards a decay described by $a_1\cos(2k_F r_T + \delta_1)/r_T$ takes place. This is shown in FIG. 4 (b), where one needs to take $a_2 \neq 0$ for describing $g(r_T)$ for $r_t \leq 30$. This crossover is also characterized by a phase shift of the fringes ($\delta_2 \neq \delta_1$), which can be seen in FIG. 4 (b). In order to find this crossover, we have studied how the 4 parameters of $F(r_T)$ depend on t_d (FIG. 4 (c)) and on U (FIG. 4 (d)), taking always for V_G the value where $g_0(V_G)$ is maximum. For having a $1/r_T^2$ decay which persists in a large domain around the nanosystem, one needs $|a_2| \gg |a_1|$. This occurs when t_d is small (FIG. 4 (c)) and $U > 1$ (FIG. 4 (d)).

In summary, neglecting electron-electron interactions and disorder in the strips, we have shown that the SGM images allow to measure the strength of electron-electron interactions inside the nanosystem. From zero temperature transport measurements, one can detect a $1/r_T^2$ decay around the nanosystem, and via $a_2(U)$, the value of U characteristic of the nanosystem can be determined. For observing this $1/r_T^2$ decay, one needs (i) interaction inside the nanosystem (dot or QPC of low electron density), (ii) large density oscillations around the tip (V_T large), and (iii) that those oscillations modify the density inside the nanosystem (r_T and t_d small, strongly coupled nanosystem and adjusted gate potential V_G). In our model, taking $g_0 \approx 1$ limits the interaction effect upon the SGM images, since g cannot exceed its limit $g = 1$. If one uses a QPC, we expect for similar reasons that biasing g_0 on the conductance plateaus makes this effect less favorable, the fluctuations of the density being limited by transverse quantization. It could explain why the ring structures found in Ref. [3] near the QPC are only seen between the conductance plateaus.

We thank S. N. Evangelou for useful comments and a careful reading of the manuscript. The support of the network "Fundamentals of nanoelectronics" of the EU (contract MCRTN-CT-2003-504574) is gratefully acknowledged.

* Present address: Department of Physics, University of Ioannina, Ioannina 45 110, Greece

[1] M. A. Topinka, B. J. LeRoy, S. E. J. Shaw, E. J. Heller, R. M. Westervelt, K. D. Maranowski, and A. C. Gossard, Science **289**, 2323 (2000).
[2] M. A. Topinka, B. J. LeRoy, R. M. Westervelt, S. E. J. Shaw, R. Fleischmann, E. J. Heller, K. D. Maranowski, and A. C. Gossard, Nature **410**, 183 (2001).
[3] N. Aoki, A. Burke, C. R. da Cunha, R. Akis, D. K. Ferry, and Y. Ochiai, J. Phys.: Conf. Series **38**, 79 (2006).
[4] E. J. Heller, K. E. Aidala, B. J. LeRoy, A. C. Bleszynski, A. Kalben, R. M. Westervelt, K. D. Maranowski, and A. C. Gossard, Nano Lett. **5**, 1285 (2005).
[5] G. Metalidis and P. Bruno, Phys. Rev. B **72**, 235304 (2005).
[6] K. J. Thomas, J. T. Nicholls, M. Y. Simmons, M. Pepper, D. R. Mace, and D. A. Ritchie, Phys. Rev. Lett. **77**, 135 (1996).
[7] Y. Asada, A. Freyn, and J.-L. Pichard, Eur. Phys. J. B **53**, 109 (2006).
[8] A. Freyn and J.-L. Pichard, Phys. Rev. Lett. **98**, 186401 (2007).
[9] A. Freyn and J.-L. Pichard, Eur. Phys. J. B **58**, 279 (2007).
[10] S. Datta, *Electronic Transport in Mesoscopic Systems* (Cambridge University Press, 1997).